Understanding functional dynamics and conformational stability of beta-glycosidases

Ben Bdira, F.

CHAPTER 2

Hydrophobic Interactions Contribute to Conformational Stabilization Endoglycoceramidase II by Mechanism-Based Probes

Abstract

Small compound active site interactors receive considerable attention for their ability to positively influence the fold of glycosidases. Endoglycoceramidase II (EGCII) from *Rhodococcus* sp. is an endo-β-glucosidase releasing the complete glycan from ceramide in glycosphingolipids. Cleavage of the β-glycosidic linkage between glucose and ceramide is also catalysed by glucocerebrosidase (GBA), the exo-β-glucosidase deficient in Gaucher disease. In this work, it is demonstrated that established β-glucoside-configured cyclophellitol-type activity-based probes (ABPs) for GBA also are effective, mechanism-based, and irreversible inhibitors of EGCII. The stability of EGCII is markedly enhanced by formation of covalent complexes with cyclophellitol ABPs substituted with hydrophobic moieties, as evidenced by an increased melting temperature, resistance against tryptic digestion, changes in ^{15}N-^{1}H transverse relaxation optimized spectroscopy spectra of the [^{15}N]-Leu-labeled enzyme, and relative hydrophobicity as determined by 8-anilino-1-naphthalenesulfonic acid fluorescence. The stabilization of the EGCII conformation correlates with the shape and hydrophobicity of the substituents of the ABPs. It is concluded that the amphipathic active site binders with aliphatic moieties act as a "hydrophobic zipper" on the flexible EGCII protein structure.

This work was published as: Ben Bdira, F., et al., Hydrophobic Interactions Contribute to Conformational Stabilization of Endoglycoceramidase II by Mechanism-Based Probes. Biochemistry, 2016. 55(34): p. 4823-4835.

Introduction

Glycosphingolipids, an important class of cellular membrane lipids, contain a ceramide, and its primary hydroxyl is glycosylated with either a glucose or galactose residue to which further sugars may be attached. Two pathways for degradation of glycosphingolipids are known to exist in nature. Non-mammalian endoglycoceramidases are able to remove in one step the entire oligosaccharide chain from the ceramide moiety. Endoglycoceramidase II (EGCII) from *Rhodococcus* sp.[1] was the first endoglycoceramidase identified (grouped in glucosyl-hydrolase family 5). Later, other non-homologous endoglycosidases degrading glycosphingolipids from leeches[2] and earthworms[3] were discovered. No mammalian endoglycoceramidase has been identified so far, although a similar enzymatic activity has been reported for rat and rabbit mammary glands[4] and human cancer cells[5]. In mammalian cells, the degradation of glycosphingolipids takes place via a very different pathway. Inside lysosomes, the subcellular compartments that specialize in the breakdown of macromolecules, terminal sugars of glycosphingolipids are removed stepwise by specific exoglycosidases, ultimately generating the free lipid, ceramide. The physiological relevance of lysosomal degradation of glycosphingolipids is illustrated by associated pathologies. Inherited defects in glycosphingolipid degrading exoglycosidases cause a number of storage diseases in humans, collectively named glycosphingolipidoses. Most prevalent among these disorders is Gaucher disease, in which deficiency of the lysosomal β-glucosidase, named glucocerebrosidase (EC 3.2.1.45, GBA), a member of glycosidase family 30 (www.cazy.org), causes accumulation of the substrate glucosylceramide. A number of GBA active site binders, called pharmacological chaperones, are being investigated as enzyme stabilizers with envisioned therapeutic application in Gaucher disease patients. One of the best studied compounds in this respect is the iminosugar isofagomine (IFG), a competitive GBA inhibitor[6,7]. The retaining β-glucosidase GBA employs a Koshland double-displacement mechanism following a $^{1}S_{3} \rightarrow {}^{4}H_{3} \rightarrow {}^{4}C_{1}$ reaction itinerary[8]. In the first displacement event, a covalent α-enzyme glucosyl intermediate is formed, with the glucopyranose moiety adopting a $^{4}C_{1}$ conformation. After binding of the substrate β-glucoside, a transition state emerges with high oxocarbenium ion character with a concomitant conformational change of the substrate in the Michaelis complex ($^{1}S_{3}$) to a $^{4}H_{3}$ half-chair[9]. It is the enzyme glucosyl intermediate state of the hydrolysis reaction that is emulated by cyclophellitol **1** (see **Figure 2.1a** for the compounds used in this study). Thus, cyclophellitol binds with high specificity to the β-glucosidase active site. Cyclophellitol **1**, first isolated from a *Phellinus* sp. culture by Atsumi and co-workers[10], irreversibly inhibits GBA by forming a stable, covalent adduct to residue Glu340[11]. The cyclophellitol epoxide is ideally positioned for acid-catalyzed nucleophilic opening involving the active side residues. As a result, a covalent enzyme-inhibitor complex is

formed (with the inhibitor now also adopting a $^4C_1$ conformation), with the ester bond much more stable and thereby irreversible compared to the acylal linkage that characterizes the enzyme-substrate covalent intermediate (**Figure 2.1b**)[9]. Substitution of the epoxide oxygen with nitrogen yields cyclophellitol aziridine **2**, an equally strong inhibitor[12]. Cyclophellitol **1** and cyclophellitol aziridine **2** functionalized to contain a fluorophore have been applied as activity-based glycosidase probes for sensitive *in vitro* and *in situ* detection of GBA molecules[11,13]. Conduritol B epoxide (CBE) **10**, an analogue of cyclophellitol lacking the C8 methylene, likewise irreversibly inhibits GBA but with lower affinity and specificity[14]. Freezing of the enzyme midway through its catalytic reaction through covalent inhibition offers an important tool for investigating the characteristics of the formed complex and elucidating which parts of the inhibitors are important for efficient stabilization activity. Despite the significant differences in their amino acid sequences, as they belong to different families of glycoside hydrolases (**Figure A1.1**), GBA and EGCII share a similar folding topology of their polypeptide chains. Both of them display a TIM barrel (triose-phosphate isomerase barrel) catalytic domain formed by $(\alpha/\beta)_8$, which makes them both members of GH-A clan (www.cazy.org). The superposition of the three-dimensional (3D) structure of the TIM barrels has a root-mean-square deviation (rmsd) of 3.1 Å for the Cα atoms [Protein Data Bank (PDB) entry 2v3e for GBA and PDB entry 2osx for EGCII] yet shows a remarkable superposition of the acid/base and the nucleophile catalytic residues, which are separated by an average distance of ~5.2 Å, consistent with their role in a double displacement mechanism with net retention of stereochemistry (see **Figure 2.2a,c**). The two proteins also have the aglycan sites in the same position relative to the active site. The analysis of the GBA crystal structure in the presence of nonyl-deoxynojirimycin (NN-DNJ), a potent inhibitor of GBA, shows that the aliphatic tail of the substrate is accommodated within a narrow hydrophobic channel where it interacts with residues Leu241, Phe246, Tyr313, Leu314, and Tyr244. Similarly, the ceramide moiety of GM3 ganglioside, the natural substrate for EGCII, makes several hydrophobic interactions with residues Leu180, Tyr182, Ile183, Phe235, Ala275, Ile276, Tyr306, and Leu308 (**Figure 2.2b,c**). In view of the similarities between the two protein binding sites, it is not surprising that NN-DNJ can also inhibit EGCII and fits well in the active site of the EGCII crystal structure (PDB entry 2OSX)[15] (**Figure 2.2c**). The GBA glycan binding site is much narrower than that of EGCII, which allows GBA to accommodate only a single glucose ring, precluding the binding of longer saccharide moieties and suggesting an explanation for the different exo and endo hydrolysis specificities for GBA and EGCII, respectively. The location of the reactive residues and primary sugar is, however, essentially the same in both active sites, suggesting that the mechanism of cleavage of the β-glycosidic linkage connecting glucose and ceramide is the same. The analogies between the two retaining β-glucosidases stimulated us to test the impact of a series of mechanism-based irreversible inhibitors known to bind covalently in the active site of GBA on EGCII conformational stability.

Here, it is demonstrated that in its free state in solution EGCII is thermolabile and highly flexible. An equilibrium between monomeric and dimeric states is observed for the resting state enzyme, because of the large solvent-exposed hydrophobic surface area of EGCII. Upon formation of the complex with the amphiphilic cyclophellitol analogues (**4-8**), marked stabilization and rigidification are observed, correlating with the lipophilic potential of the compounds. No changes are observed in the protein stability or rigidity after incubation with non-hydrophobic compounds (**1** and **2**). These findings demonstrate the importance of the length and shape of the non-glycan moiety of substituted cyclophellitols for the enzyme stabilization.

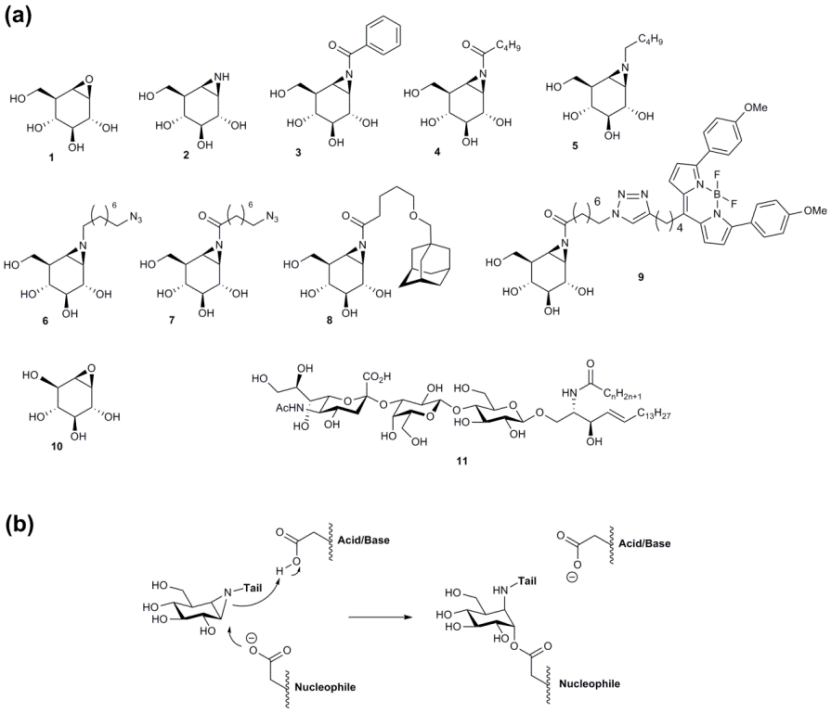

Figure 2.1. (**a**) Structures of β-glucoside-configured cyclophellitols used and (**b**) Mechanism-based inactivation of β-glucosidases by covalent binding to a catalytic nucleophile.

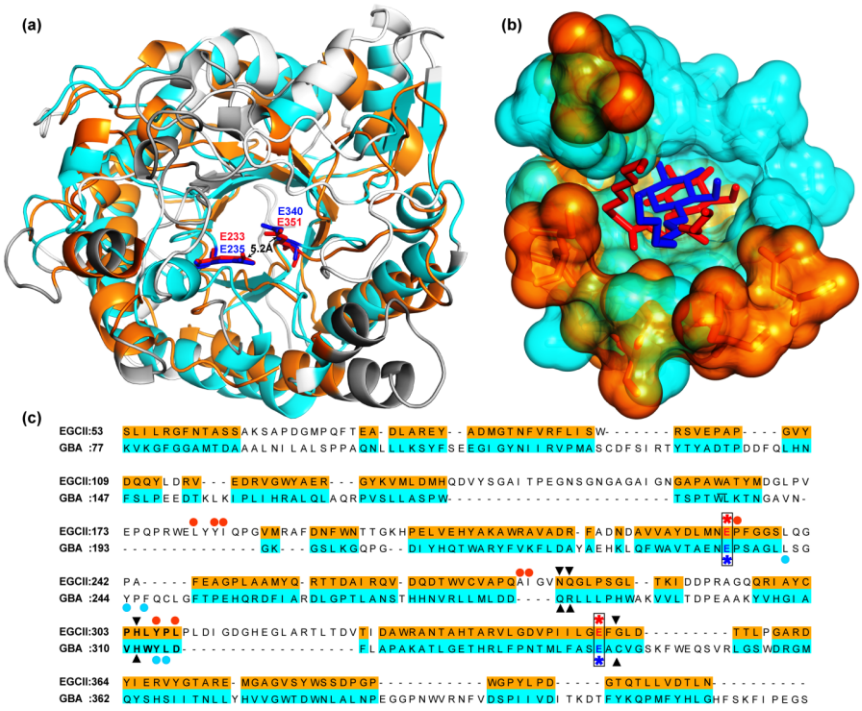

Figure 2.2. Comparison of the folding topology and aglycan binding sites of GBA and EGCII. (**a**) Structural alignment of the TIM barrel catalytic domain of EGCII (orange cartoon) and GBA (cyan cartoon) using the jFATCAT algorithm[59] (RCSB comparison tool). The acid/base and nucleophile catalytic residues are shown as sticks and colored red for EGCII and blue for GBA. For the sake of clarity, non-overlapping loops were hidden. (**b**) Aglycan binding site cavities of EGCII (orange) and GBA (cyan) as observed in the superposition shown in panel **a**. The surface of the residues interacting with the aliphatic tail of the ligands is shown; β-D-glucose-ceramide (in EGCII) is colored red and NN-DNJ (in GBA) blue. (**c**) Primary sequences of EGCII and GBA with the structurally homologous parts highlighted in orange and cyan, respectively. Acid/base catalytic residues are marked with stars and a black box. Hydrophobic residues interacting with the NN-DNJ alkyl chain and the ceramide moiety of GM3 are marked with cyan and orange circles, respectively. Non-hydrophobic interacting residues within the aglycan binding sites are marked by black triangles.

Results

Readouts for Active EGCII Molecules. It is first identified convenient readouts for active EGCII molecules. It is determined whether 4-methylumbelliferyl lactoside (4MU-Lac) is a suitable fluorogenic substrate for recombinant EGCII. This proves to be the case. The enzyme exhibits an optimal activity at pH 5.5 (**Figure 2.3a**), with hydrolysis occurring in a time-dependent manner (**Figure 2.3b**). Next, it is demonstrated that EGCII can be labeled in a mechanism-based manner by a β-glucoside-configured cyclophellitol **10** and cyclophellitol-aziridine substituted with a BODIPY fluorophore **9** (**Figure 2.3c**).

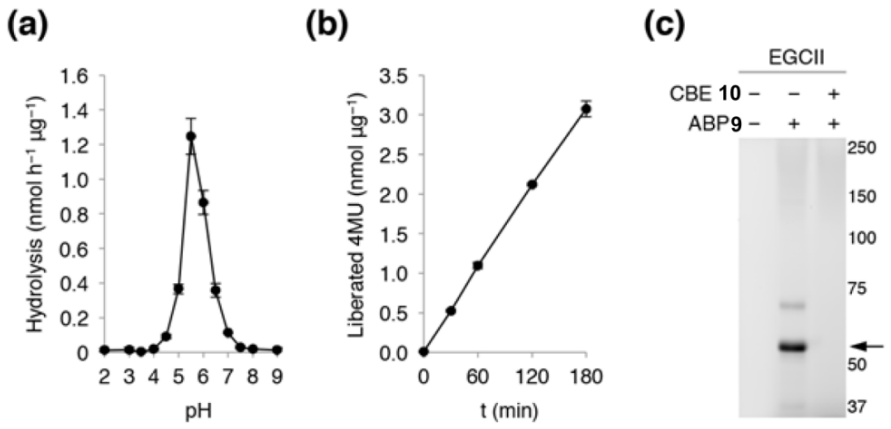

Figure 2.3. Read-outs of active EGCII molecules. **(a)** Hydrolysis of 4MU-Lac by EGCII across a pH range, at 17 °C in 150 mM McIlvaine's buffer. **(b)** Time-dependent liberation of 4MU from 4MU-Lac by EGCII at 17 °C and in 150 mM McIlvaine's buffer pH 5.5 **(c)** Labeling of EGCII with cyclophellitol-aziridine ABP **9** at pH 5.5 and 17 °C and its competition by pre-incubation with CBE **10** in 150 mM McIlvaine's buffer pH 5.5. The main EGCII protein band is marked with an arrow.

Thermal stability of EGCII

Under optimal conditions for enzymatic activity [150 mM McIlvaine's buffer (pH 5.5)][16] was monitored by recording the temperature dependence of the dichroic signal at 222 nm and applying a range of heating rates from 1 to 5 °C/min (**Figure 2.4a**). The obtained unfolding curve at a heating rate of 1 °C/min shows an apparent T_m of 42 °C, close to the enzyme optimal catalytic temperature (37 °C) (**Figure 2.4b**)[1]. The apparent T_m value depends on the scanning rate, suggesting an irreversible denaturation process toward aggregation, which is visible by eye due to the turbidity of the protein solution. The unfolding kinetics of EGCII at 37 °C (pH 5.5) were determined by recording a CD spectrum every 10 min for 50 min. EGCII shows an exponential decay of its ellipticity signal at 222 nm with a half- life of ~10 min and forms a visible aggregate. The enzymatic

activity was also tested with 4MU-Lac as a substrate. A parallel decay was observed (**Figure 2.4c**), correlating unfolding kinetics with loss of activity. During the kinetic unfolding, the amount of residual active protein was also followed by labeling with the activity-based probe compound **9** (**Figure 2.4c**, bottom panel). A similar decay of the fluorescently labeled EGCII over the incubation time was observed. EGCII denaturation was also followed at 25 °C by CD (**Figure 2.4d**). At this temperature, the enzyme's activity is close to optimal (**Figure 2.4b**). At 25 °C [150 mM McIlvaine's buffer (pH 5.5)], EGCII is stable with no changes in its secondary structure and its active state as monitored by ABP (**Figure 2.4d**, bottom panel). These results show that EGCII is a thermolabile protein with an apparent T_m of 42 °C at a heating rate of 1 °C/min and tends to form an aggregate as a final step in the irreversible unfolding process. Therefore, for experiments requiring prolonged incubations, it is practical to work at 25 °C.

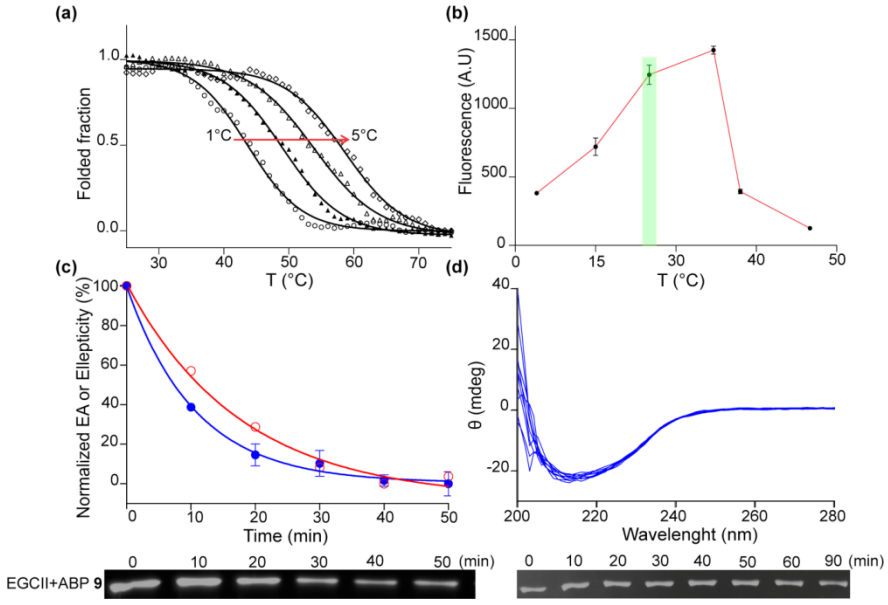

Figure 2.4. Thermodynamic stability of EGCII. (**a**) Thermal denaturation curves of EGCII at varying scanning rates (1-5 °C/min), at a protein concentration of 5 μM. (**b**) Temperature dependence of EGCII activity toward 4MU-Lac in 150 mM McIlvaine's buffer (pH 5.5), with an incubation time of 1 h. The activity at 25 °C is highlighted by the green rectangle; the error bars represent the standard deviations of a duplicate experiment. (**c**) Decays over time of the ellipticity at 222 nm (red empty circle and curve), the specific activity (blue filled circle and curve), and SDS-PAGE of ABP labeling of EGCII samples at 37 °C in 150 mM McIlvaine's buffer (pH 5.5) (bottom panel). The red and blue curves are exponential decay fits of the ellipticity and enzymatic activity (EA), respectively. The half-life decays are 12 min (ellipticity) and 7 min (enzymatic activity). The error bars represent standard deviations of a duplicate experiment. (**d**) EGCII kinetic stability at 25 °C monitored by circular dichroism spectra (blue lines), recorded every 10 min for 90 min, and SDS-PAGE of ABP selective labeling of EGCII (bottom panel).

EGCII flexibility and conformations in solution

Limited proteolysis with trypsin at a trypsin: EGCII ratio of 1:100 was employed to investigate the flexibility of EGCII in solution. Proteolysis under different conditions and as a function of incubation time was analyzed via SDS-PAGE. At 25 °C, directly after trypsin addition, an additional band rapidly appears on the gel close to the intact protein. This could result from cleavage of one of the flexible ends of the protein. After incubation for 10 min, approximately 50% of the protein has been digested with the appearance of two major protein fragments with apparent molecular weight of 34 and 25 kDa (**Figure 2.6a**). These fragment species remain relatively resistant to °C, the protein was fully digested into these two bands within 10 min, the digestion already being observed immediately upon addition of the protease (time zero) (**Figure 2.6c**). The peptic fragment pattern is similar at 37 and 25 °C, suggesting that digestion occurs at the same position in the polypeptide. To correct for the difference in trypsin activity at 25 and 37 °C, the digestion at 25 °C was conducted by adding 3 and 10 times more trypsin. The tryptic pattern of EGCII was not affected by the additional trypsin activity (**Figure 2.5**). The subsequent rapid disappearance of the tryptic fragments at 37 °C, as compared to that at 25 °C, suggests that at the lower temperature the nicked polypeptide remains folded, whereas at higher temperature it unfolds, allowing further proteolysis of the two fragments. We tried to identify the site of digestion by mass spectrometry.

The in-gel digestion and analysis by LC/MS of the produced tryptic fragments suggested that the major digestion occurs after Arg332. However, LC/MS of the intact fragments (that is, without further digestion into smaller peptides) suggested that the major digestion site is located after the preceding arginine residue at position 321 (observed mass for C-terminal fragment 18622 Da, expected 18624 Da). It is concluded that either or both of these arginines represent the primary cutting site. Interestingly, in the EGCII crystal structure, both arginines are located in a long, well-structured α-helix (**Figure 2.6e**). In a modeling study, Hubbard et al. concluded that a local disorder or unfolding of the protein polypeptide chain of at least 12 residues is required to allow access into a protease active site[17]. Therefore, those results suggest that this part of the protein is less structured in solution than in the crystalline state. In the presence of the detergent lauryl glucoside (**Figure 2.6b**) or Triton X-100 (**Figure 2.6d**), the protein is strikingly resistant to tryptic digestion. It has been reported that the used surfactants have no inhibitory effects on trypsin[18]. This tryptic resistance of the protein in the presence of detergents could be due to interaction with the micelles, shielding the protein surface, leading to a more rigid and compact structure. Moreover, lauryl glucoside has an amphiphilic structure quite similar to that of EGCII natural substrates **11** (**Figure 2.1a**), and thus, it might interact with the binding pocket of the protein, stabilizing it in a rigid conformation (see below). Crystals of ECGII were obtained in the presence of 1% (v/v) Triton X-100, 10% (v/v) glycerol, and 25% (w/v) PEG[19]. The possibility that under these conditions, and because of crystal

packing effects, the protein could adopt a rigid conformation that is not representative of the lowest-energy state present in solution cannot be excluded.

Next, EGCII in solution was studied by size exclusion chromatography (SEC) to monitor changes in the hydro- dynamic dimensions accompanying unfolding, dimerization, or conformational changes of globular proteins in solution[20,21]. It is observed that EGCII elutes as two fractions from the SEC column (P1 and P2) with elution volumes of 8.5 and 9.5 mL, respectively. The integration of the chromatogram peaks area yields percentages of 30 and 70% for peaks 1 and 2, respectively (**Figure 2.7a**). The re-injection of the extremity of the collected fractions of the two peaks shows an exchange between the two states of the protein even at low concentrations (**Figure 2.7c**). The enzymatic activity of both peak fractions was the same within error (**Figure 2.7b**). They also exhibit the same molecular weight on SDS-PAGE. Therefore, both fractions represent a native and active state of EGCII. Native PAGE analysis of EGCII shows two bands, and staining of the gel with ABP 9 confirms that the enzyme in both of the bands is active (**Figure 2.7d**). The analysis of the molecular weight of the eluted peaks with SEC-MALLS yields an *M*w of 100 kDa for P1 and an *M*w of 50 kDa for P2 (**Figure A1.2**), providing more evidence of a monomeric state and a dimeric state of the protein. Thus, it is concluded that EGCII is in equilibrium between monomeric and dimeric states in solution.

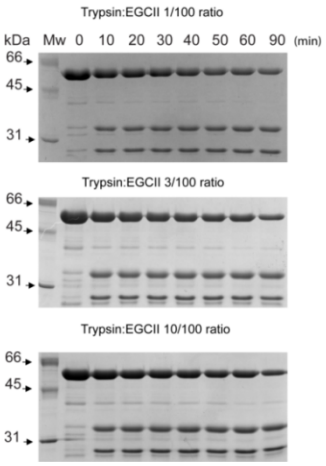

Figure 2.5: Tryptic digestion of EGCII at different ratios: Tryptic digestion of EGCII with trypsin from bovine pancreas (Sigma) with Trypsin: EGCII ratios 1:100, 3:100, 10:100 (by weight) in 150 mM McIlvaine's(citrate/phosphate) buffer pH 5.5 at 25°C.

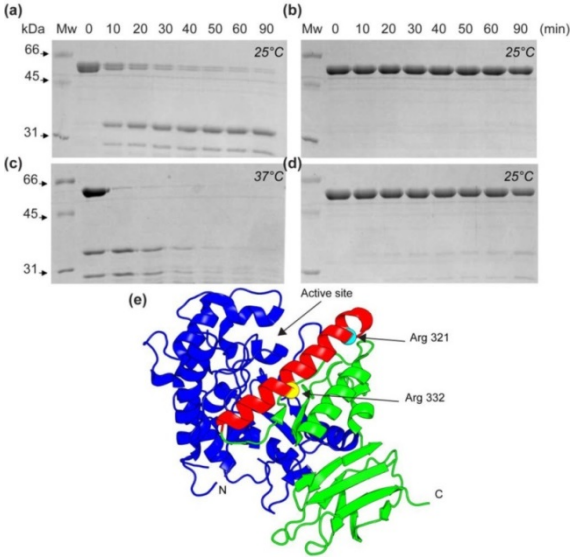

Figure 2.6. Time course of tryptic proteolysis of EGCII analyzed by SDS−PAGE. Tryptic proteolysis was performed at an E:S ratio of 1:100 (by weight) in 150 mM McIlvaine's buffer (pH 5.5) at 25 °C (**a**), at 25 °C in the presence of 1% lauryl glucoside (**b**), at 37 °C (**c**), and at 25 °C in the presence of 1% Triton X-100 (**d**). Samples (5 µg) were taken from the reaction mixture every 10 min and analyzed via 10% SDS−PAGE followed by protein staining. (**e**) Major trypsin cleavage sites (Arg321 and Arg332 in the red helix) identified by mass spectrometry and depicted in EGCII 3D structure (PDB entry 2osw)[19]. N-Terminal and C-terminal protein fragments are colored blue and green, respectively.

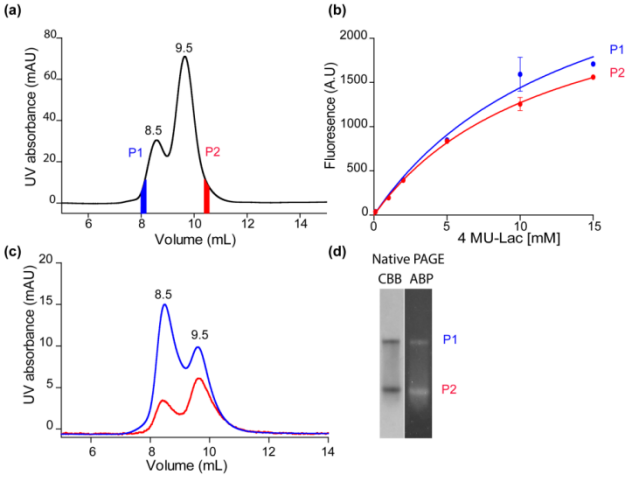

Figure 2.7. EGCII solution state analysis by size exclusion chromatography and native PAGE. (**a**) EGCII size exclusion chromatogram in 20 mM Tris-HCl and 150 mM NaCl (pH 7.6). The elution volumes of the peaks are indicated. (**b**) Enzymatic activity of eluted fractions P1 and P2 using 4MU-Lac as a substrate. The error bars represent the standard deviations of two experiments. (**c**) Size exclusion chromatograms of eluted fractions P1 (blue) and P2 (red). (**d**) Native gel analysis of the EGCII sample in Tris buffer, stained with Coomassie Brilliant Blue (CBB) and the activity-based probe (ABP) **9**.

EGCII complexed with *N*-alkyl azide-substituted cyclophellitol aziridine (compound 6)

Because EGCII was found to irreversibly react with cyclophellitol aziridines, the impact of cyclophellitol derivatives on the biophysical properties of EGCII was studied. For this, compound **6** was used, an *N*-alkylated cyclophellitol aziridine functionalized with an azide. The effects of compound **6** on the thermodynamic properties of EGCII were investigated by measuring the apparent T_m of the complex. A pronounced increase in the apparent T_m of 12 °C was observed (**Figure 2.8a**). Such an increase is usually accompanied by changes in the protein structure and rigidity[22,23]. The occurrence of conformational changes of EGCII upon complex formation was probed by comparing ^{15}N-^{1}H TROSY spectra of the free and bound states. EGCII contains 38 leucine residues that were used as probes to detect conformational changes. In the free form, only a few resonances are observed (**Figure 2.8b**), which are very intense, suggesting that some leucine residues are in highly flexible regions whereas many others experience slower mobility, on the millisecond to microsecond time scale, which results in broadening of their resonances due to chemical exchange processes. For the EGCII-**6** complex, additional peaks with more spectral dispersion are observed, suggesting rigidification of regions of the enzyme. The effect of these conformational changes on the solvent-accessible hydrophobic surface of EGCII was monitored by ANSA, as an extrinsic fluorescence probe, which interacts with the exposed hydrophobic areas of the protein. The results show an 8-fold decrease in exposed protein hydrophobicity between the enzyme in the free form and that bound to compound **6**, as determined from the changes in ANSA fluorescence curve slopes (**Figure 2.8c**). The change in the accessible hydrophobic surface is accompanied by a shift in the protein equilibrium between the dimeric and monomeric state toward the monomeric state, as demonstrated by the single elution peak in SEC (**Figure 2.8d**). This suggests that the dimerization is due to intermolecular interactions between the exposed hydrophobic surfaces of the protein. Additionally, the effect of complex formation on EGCII flexibility was tested by trypsin digestion at 25 and 37 °C. At 25 °C, the EGCII-**6** complex is more resistant to proteolytic activity, compared to the protein free state, as shown by SDS-PAGE (**Figure 2.9a**). At 37 °C, the protein is still digested into two bands. However, these two bands persist during the incubation time (**Figure 2.9c**), contrary to what was observed for the free protein. This latter peptic profile resembles that seen in the free state at 25 °C. The peptic fragments were analyzed by Western blotting with an anti-His tag antibody against the C-terminal histidine tag of EGCII. The blot confirms that the lower band contains the C-terminal fragment of the protein (**Figure 2.9b**). The same peptic pattern is observed when the protein is labeled with activity-based probe 9. The lower band is the part of the protein that contains covalently bound ABP **9**, presumably to the nucleophile Glu351 (**Figure 2.9d**). To investigate the EGCII-**6** complex peptic fragment, the trypsin-cleaved

and uncleaved EGCII samples were analyzed by SEC. Their chromatograms show the same elution volume for a single peak, and also single bands are observed via native gel electrophoresis (**Figure 2.9e,f**). These observations support the conclusion that after digestion the two protein fragments stick together forming a strong noncovalent complex. On SDS-PAGE, two bands were observed due to the dissociation of the complex under the denaturing conditions (**Figure 2.9f**). Therefore, it could be speculated that the hydrophobic interaction between the two nicked fragments is the main force that keeps the complex together. This hydrophobic interaction is likely enhanced by the aliphatic tail of the irreversible inhibitors. On the basis of these observations, it can be concluded that in its complexed state EGCII experiences pronounced conformational changes, as seen from its ^{1}H-^{15}N HSQC-TROSY spectrum and the measured accessible hydrophobic solvent. Additionally, an increase in trypsin resistance was observed, although the trypsin cleavage site remains accessible. This conformation of the protein may represent a closed and rigid state that could be stabilized by the hydrophobic interaction between the aliphatic tail of the irreversible inhibitor and the hydrophobic part of the substrate binding site.

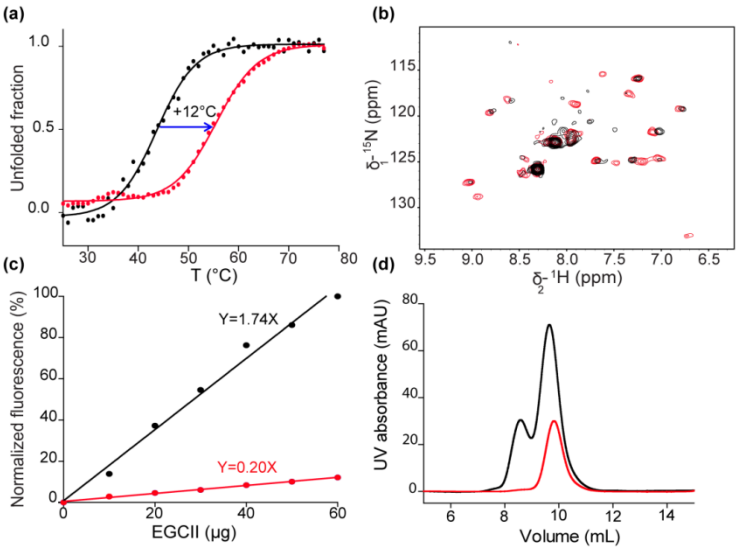

Figure 2.8. Effects of compound 6 on EGCII structure and thermal stability. (**a**) Thermal denaturation at pH 5.5 monitored by CD spectroscopy with a heating rate of 1 °C/min. The fitted apparent Tm values of the EGCII free state (black) and the EGCII-6 complex (red) were 43 and 55 °C, respectively. (**b**) ^{15}N-^{1}H TROSY spectra of [^{15}N]-Leu-labeled EGCII in the free (black) and bound (red) states. (**c**) Relative solvent-accessible hydrophobic surface of EGCII free (black) and bound (red) states, determined by ANSA fluorescence. The lines represent a linear fit through the origin with the indicated fitted slopes. (**d**) Size exclusion chromatograms of EGCII free (black) and covalently bound (red) states.

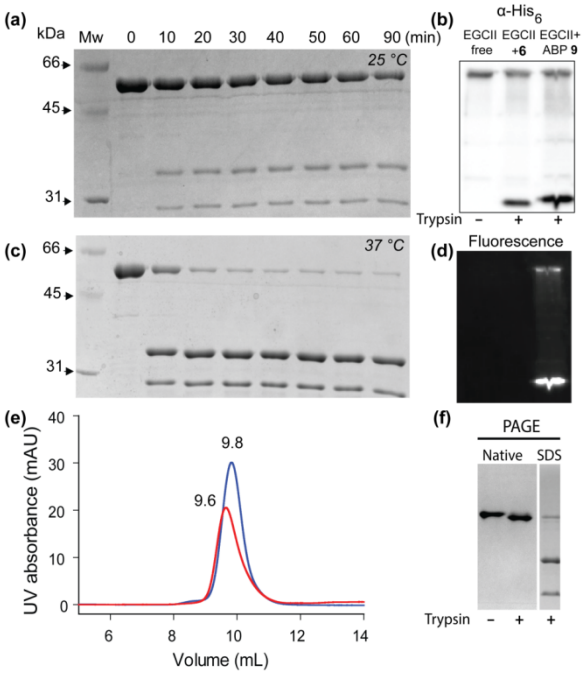

Figure 2.9. Rigidification of EGCII by compound **6**. EGCII-**6** complex peptic fragment pattern at 25 °C (a) and 37 °C (**c**) on 10% SDS−PAGE. (**b**) Anti- histidine tag Western blot membrane of digested EGCII in its free state and bound to compound 6 or ABP 9. (**d**) Fluorescence image (Cy3) of the anti- histidine tag blot showing the fluorescence of ABP. (**e**) Size exclusion chromatograms of trypsin-treated (red) and untreated (blue) EGCII-**6** complex. The elution volumes of the peaks are indicated. (**f**) Untreated EGCII-**6** complex and EGCII-**6** treated with trypsin analyzed under native and denaturing electrophoresis conditions.

Correlation between EGCII stabilization and the lipophilic potential of cyclophellitols

A series of cyclophellitol aziridines *N*-alkylated or *N*-acylated with different lipophilic moieties (**Figure 2.10a**) were screened and the effects on EGCII melting temperature monitored by CD. Compounds **1** and **2** have no effect on the EGCII apparent T_m, in contrast to compounds **4**-**8**, for which an increase in the apparent T_m was observed with a maximal shift of 14.5 °C obtained with compound **8**, containing an adamantane moiety (**Figure 2.10b**). A correlation between the molecular lipophilic potential of the compounds and the increase in EGCII melting temperature is observed. This correlation can be explained by the more compact and rigid conformation adopted by the protein upon the interaction with the cyclophellitol aliphatic tags. Next, the solvent-accessible hydrophobic surfaces (SAHSs) of EGCII-cyclophellitol/cyclophellitol aziridine complexes were measured by ANSA (**Figure 2.10c**), and a decrease in EGCII SAHS was observed with an increase in inactivator lipophilicity. To highlight this correlation, the SAHS of the complexes is plotted against the theoretical "log *P*" of the compounds (**Figure 2.10d**). The plot suggests that with an increasing tag hydrophobicity, the protein

adopts a more closed and compact conformation. An exception is observed for compound **3**, which could be due to its bulky aromatic ring that may cause steric hindrance in the narrow hydrophobic channel of the substrate binding pocket. On the basis of these results, it is concluded that the shape and length of the aliphatic tail, and therefore its molecular lipophilic potential, are key factors for rigidification and stabilization of EGCII.

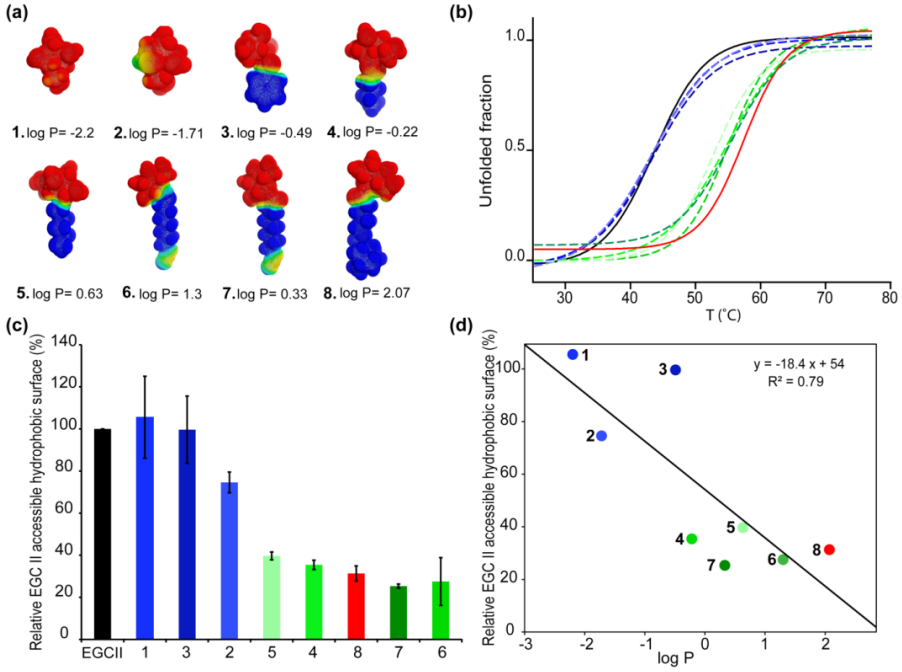

Figure 2.10. EGCII-cyclophellitol-aziridine derivative complexes. (**a**) Molecular lipophilic potential of cyclophellitol-aziridine derivatives as visualized using MLP Tools, a PyMOL plugin[60]. (**b**) Fits of thermal denaturation curves of the different EGCII compound complexes, monitored by circular dichroism at pH 5.5 (the colors agree with those in panels c and d, and experimental data points were omitted for the sake of clarity). (**c**) Effect of the tested compounds on the relative EGCII solvent-accessible hydrophobic surface monitored by ANSA fluorescence. (**d**) Correlation between the calculated log *P* of the different tested compounds and the relative solvent-accessible hydrophobic surface of EGCII compound complexes. The free EGCII solvent-accessible hydrophobic surface was set to 100%.

Discussion

The interaction of a ligand binding protein with its cognate substrate usually induces changes in the protein thermal stability, resulting in a shift of the observed melting temperature (T_m). This phenomenon is widely exploited as a tool to identify potential binders for scientific and medicinal applications[24,25]. For instance, this approach found successful application in the identification of target inhibitors in drug screening and for decrypting unknown protein functions. As an illustrative example, ligand-induced protein stabilization was used to identify inhibitors against human serine/threonine kinases. It was found that compounds that enhanced protein thermostability have a higher inhibition activity[26]. Another example is the elucidation of a protein function of an essential gene from *Streptococcus pneumoniae* using a thermofluor screening assay[27]. A library of 3000 compounds was screened against the unknown functional protein, and two hits were found to increase the protein thermal stability by 25 and 5 °C. The shifts of the protein melting temperature correlated with the ligand dissociation constant (K_d values of ≈50 pM and ≈2.5 μM, respectively). The protein was identified as a nucleoside diphospho-keto-sugar aminotransferase[27]. Ligand-induced protein stabilization can also be attained by changes of the protein conformational flexibility[28-30]. By studying the interaction between ANSA derivatives and BSA, Celej and co-workers found that binding of ligand to the protein induces an increase in protein conformational rigidity that correlates with thermostability[30]. Rigidification upon ligand binding is used to screen for small compounds that assist protein refolding and prevent their aggregation[31] or for specific active site binders that stabilize the folded state of a protein and improve its functionality[32]. The latter compounds are called pharmacological chaperones and have potential application in drug discovery for rescuing protein activity in several misfolding diseases[33-36]. As a representative example, a deficiency of GBA activity represents the etiology of Gaucher disease, the most common lysosomal storage disorder[37]. This deficiency can be due to various point mutations, destabilizing the protein fold and disrupting cellular tracking. It has been reported that active site binders restore to some extent the activity of lysosomal retaining β-glucosidase GBA mutants by stabilizing the folded conformation of the protein. For instance, IFG increased GBA thermal stability at neutral pH by 8.7 °C and improved protein traffcking of the N370S GBA mutant, resulting in an increase in GBA cellular levels in Gaucher patient tissues, including brain[38]. Additionally, oral administration of IFG increased GBA L444P mutant activity in mice up to 5-fold[7]. Several lipophilic IFG derivatives proved to have a higher affinity and chaperoning activity toward GBA mutants[39-42]. In connection to these findings, irreversible inhibitor cyclophellitol and its aziridine derivatives were also found to be effective mechanism-based ligands against retaining β-glucosidases[43-45]; therefore, they were used to study the kinetics and structural basis of β-glucosidase inhibition[46]. In the

work presented here, on the basis of the similarity of the structural topology between β-glucosidases GBA and EGCII as well as of their target of catalysis, the β-glucosidic linkage in glucosylceramide, it was speculated that cyclophellitol derivatives binding covalently to the catalytic nucleophile of GBA might also react with EGCII. The observation that EGCII is indeed irreversibly inhibited by cyclophellitol derivatives opened new possibilities for research on the enzyme. The factors influencing the conformational stability of EGCII were investigated with several biophysical and biochemical techniques, with emphasis on the effect of occupancy of the active site by cyclophellitols. This investigation led to a number of findings warranting further discussion. The thermostability study of EGCII by circular dichroism indicated that the protein has an apparent midpoint of the unfolding transition of 42 °C with an irreversible unfolding process, forming an aggregate as a final state. The isothermal denaturation of EGCII at 37 °C, which represents its optimal catalytic temperature, shows that the protein has a short half-life of 10 min, unlike what was observed at 25 °C where the protein shows a remarkable kinetic stability. These findings differ from those reported by Ito and co-workers. They found that the protein has a thermal stability of 60 min at 37 °C at the same pH[1]. An explanation for this discrepancy is presently not available; the buffer conditions were not reported, so they may have deviated from the ones used here. The noted thermolability of EGCII could stem from its 3D structure containing several flexible regions without a well-packed hydrophobic core[19]. Analysis of EGCII flexibility in solution by proteolysis shows that the protein is susceptible to trypsin and has a major cleavage site localized in an α-helix in the crystal structure. It has been reported that protease cleavage sites for a variety of proteins of known 3D structure never occur in α-helices, but largely in loops[47]. Therefore, it is speculated that this region in solution is either highly flexible or locally disordered. In the presence of detergents, this cleavage site becomes inaccessible to the trypsin and adopts a more structured conformation, as observed in the crystal structure of the protein. This local conformational flexibility, in combination with the high positive charge in this region, could play a crucial role in membrane association of EGCII, required to exert its enzymatic activity toward glycosphingolipids. The fact that EGCII processes a wide range of substrates[24], which requires a high flexibility and plasticity of the substrate binding site, may also explain its flexible behavior in solution. Protein flexibility may also be important in protein-protein complex formation. EGCII has an activator of 69 kDa that increases the catalytic activity of the enzyme against gangliosides in the absence of detergents under *in vitro* conditions[48]. It could be that protein flexibility is necessary for protein-activator complex formation via an induced-fit mechanism. EGCII has a typical TIM (triose-phosphate isomerase) barrel folding pattern with a $(\beta/\alpha)_8$ N-terminal domain and a β-sheet C-terminal domain[27]. The function of the β-sheet domain is unclear, even though it is highly conserved in different families of retaining β-glucosidases. The attempt to express only the catalytic domain to no avail, and all of the produced protein was found in inclusion bodies. This observation,

combined with the high flexibility of the catalytic domain, supports the hypothesis that this domain not only is necessary for the stability of the catalytic domain but also may play a crucial role as an internal chaperone to guide the folding of the catalytic domain. The dramatic stabilization and rigidification of EGCII upon complex formation with the irreversible inhibitors are caused by the hydrophobic interaction with their aliphatic tail. A correlation between the molecular lipophilic potential of the tested compounds and the decrease in the solvent-accessible hydrophobic surface was observed. When accommodated into the enzyme binding pocket, the hydrophobic moieties of the compound appear to function as a "hydrophobic zipper". This interaction makes the protein more rigid but with the preservation of the trypsin cleavage site. After cleavage, the two fragments were shown to stay together in a noncovalent complex, mediated by the hydrophobic interactions with the aliphatic tail of the irreversible inhibitor. A similar mechanism of binding pocket occupancy effects was observed for the complex between renin, an aspartic protease playing a key physiological role in the regulation of blood pressure, and a nonpeptidomimetic inhibitor, showing dramatic structural changes in renin. In this case, a movement of protein flexible loops of the binding pocket was observed and further changes in the protein around the bulky lipophilic substitutes of the inhibitors were seen. The lipophilic substitutes and hydrophobic side chains in renin act to form a new compact hydrophobic region within the protein[49]. A stabilization and rigidification effect was also observed in the case of the covalent modification of the β-(1-4)-glycosidase Cex catalytic domain, from the soil bacterium *Cellulomonas fimi*, with the mechanism-based inhibitors 2,4-dinitrophenyl 2-deoxy-2- fluoro-β-cellobioside. The free state of the Cex catalytic domain was markedly stabilized upon formation of the glycosyl−enzyme intermediate with an increase in its T_m of 10.5 °C. This protein stabilization was accompanied by a distinct thermolysin proteolytic resistance, with no proteolysis of the glycosyl-enzyme complex occurring, even after incubation for 50 h at 50 °C[50].

Conclusion

In conclusion, EGCII was used as a research model to investigate the effects of occupancy of the active site by cyclophellitol analogues with variable lipophilic potential. The hydrophobic interaction plays a decisive role in the protein-inhibitor complex, promoting rigidification of the protein and conformational stability. In theory, endoglycoceramidases could be employed to treat a number of inherited glycosphingolipidoses caused by deficiency in a lysosomal exoglycosidase. Insight into factors influencing the conformational stability of endoglycoceramidases is one important prerequisite for their design as successful therapeutic agents.

Experimental procedures

General synthesis

All reagents and solvents were of commercial grade and used as received unless stated otherwise. Tetrahydrofuran and dichloromethane were stored over flamedried 3 Å molecular sieves. All reactions were performed under an inert atmosphere unless stated otherwise. Solvents used for flash chromatography were of pro analysis quality. Reactions were monitored by TLC analysis using aluminum sheets precoated with silica gel 60 with detection by UV absorption (254 nm) and by spraying with a solution of $(NH_4)_6Mo_7O_{24} \cdot H_2O$ (25 g/L) and $(NH_4)_4Ce(SO_4)_4 \cdot H_2O$ (10 g/L) in 10% sulfuric acid, followed by charring at ~150 °C or by spraying with 20% sulfuric acid in ethanol followed by charring at ~150 °C. Column chromatography was performed using Screening Device silica gel in the indicated solvents. ^{1}H-nuclear magnetic resonance (NMR), ^{13}C NMR, COSY, and HSQC spectra were recorded on Bruker DMX-400 (400/100 MHz), Bruker AV-400 (400/100 MHz), and Bruker AVIII-600 (600/150 MHz) spectrometers in the given solvent. Chemical shifts are reported as δ values in parts per million relative to the chloroform residual solvent peak, tetramethylsilane (TMS) as an internal standard, or the deuterated solvent signal for CD_3OD. All given ^{13}C spectra were proton-decoupled. High-resolution mass spectra were recorded with an LTQ Orbitrap instrument (ThermoFinnigan). LC/MS analysis was performed on an LCQ Adventage Max (ThermoFinnigan) ion trap spectrometer (ESI+) coupled to a Surveyor high-performance liquid chromatography (HPLC) system (ThermoFinnigan) equipped with a C18 column (Gemini, 4.6 mm ×50 mm, 3 µ m particle size, Phenomenex) using buffers A (H_2O), B (acetonitrile in MeCN), and C (50mM NH_4OAc). For reverse phase HPLC purifications, an Agilent Technologies 1200 series instrument equipped with a semi preparative Gemini C18 column (10 mm ×250 mm) was used. The applied buffers were 50 mM NH_4HCO_3 in H_2O (buffer A) and MeCN (buffer B). Compound **6** was synthesized according to a published report[51]. Compounds **1**-**5** and **7** and cyclophellitol-aziridine ABP **9** were prepared as described previously[52].

Synthesis of compound 8

N-Ethoxycarbonyl-2-ethoxy-1,2-dihydroquinoline (EEDQ) (79 mg, 0.32 mmol) and 6-*O*-adamantanemethyl-6-hydroxyhexanoic acid X (85 mg, 0.32 mmol) were dissolved in anhydrous DMF (0.32 mL) and stirred at room temperature for 2 h (**Scheme 2.1**). The resulting dissolved mixed anhydride (160 µL) was added to cyclophellitol-aziridine **2**[17] (35 mg, 0.2 mmol) in dry DMF (1.2 mL) at 0 °C and stirred for 30 min. At this time, an additional batch of mixed anhydride (160 µL) was added. The resulting mixture was stirred at 0 °C for 2 h. The reaction was quenched with MeOH (1 mL), and the mixture

was concentrated *in vacuo*. Then the crude product was purified by semipreparative reverse HPLC [linear gradient from 38 to 47% B in A, 12 min; solutions used, H_2O (A) and MeCN (B)], and the fractions were lyophilized yielding 8 as white powder (21 mg, 0.05 mmol, 25% yield): 1H NMR (400 MHz, MeOD) δ 4.09 (d, $\mathcal{J}$ = 10.4, 4.4 Hz, 2H), 3.72−3.66 (m, 2H), 3.414 (t, $\mathcal{J}$ = 6.4 Hz, 2H), 3.23 (dd, $\mathcal{J}$ = 10.0, 8.0 Hz, 1H), 3.10−3.02 (m, 2H), 2.74 (d, $\mathcal{J}$ = 5.6 Hz, 1H), 2.55−2.51 (m, 2H), 2.01−1.95 (m, 4H), 1.77−1.66 (m, 8H); 1.64−1.56 (m, 8H);13C NMR (100 MHz, MeOD) δ 188.5, 83.0, 79.1, 73.4, 72.2, 69.4, 63.6, 45.3, 42.4, 41.1, 40.8, 38.3, 36.6, 35.2, 30.1, 29.9, 29.8, 22.9; LC/MS t_R 7.87 min (linear gradient from 10 to 90% B in 15 min); ESI-MS *m/z* 424.4 (M + H)+; HRMS calcd for $C_{14}H_{17}NO_4$ (M + H+) 424.26936, found 424.26921.

Scheme 2.1. Synthesis of Compound **8**

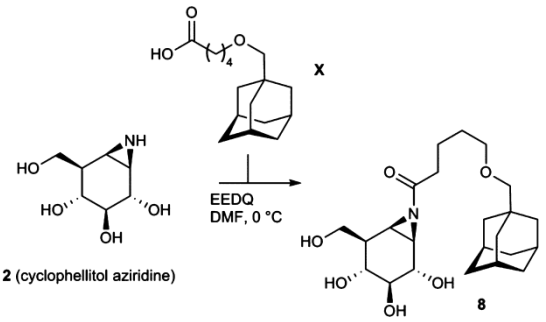

Production and purification of recombinant EGCII

The gene encoding EGCII from *Rhodococcus* sp. strain M777 lacking the N-terminal signal peptide sequence was subcloned into pET21a using NdeI/NotI restriction sites, introducing a C-terminal His tag. *Escherichia coli* BL21(DE3) pLysS cells were transformed with the obtained vector and cultured at 37 °C in lysogency broth containing 50 μg/mL ampicillin and 30 μg/mL chloramphenicol. Gene expression was induced with 0.5 mM isopropyl β-D-1-thiogalactopyranoside (IPTG) when the culture reached an OD_{600} of ≈ 0.6, and the incubation was continued overnight at 20 °C. The cells were harvested by centrifugation, resuspended in extraction buffer [20 mM Tris-HCl, 150 mM NaCl, and 20 mM imidazole (pH 7.6)], and sonicated. The resulting EGCII 6-His supernatant was further purified by Ni(II) affnity chromatography to > 95%, as determined by sodium dodecyl sulfate-polyacrylamide gel electrophoresis (SDS-PAGE). All the purification steps were conducted at 4 °C. [^{15}N]-Leucine isotope selective labeling of EGCII was started by culturing the transformed *E. coli* BL21(DE3) in a 50 mL culture in M9 medium overnight at 37 °C, supplemented with each amino acid (at 0.1 g/L) except leucine, as well as 125 mg/L adenosine, 125 mg/L guanosine, 125 mg/L cytosine, 50 mg/L thymine, 50 mg/L uracil, 50 mg/L nicotinic acid, and 2 g/L succinic acid. The next day, 0.5 L of this medium was inoculated with the overnight preculture and incubated at 37 °C until the OD_{600} reached ≈ 0.6. Fifteen minutes before induction, a mixture of 0.5 g of each unlabeled amino acid except leucine and 50 mg of [^{15}N]-Leucine were added to the culture[53]. Protein production was started by inducing gene expression with 0.5 mM

IPTG, and the culture was continued overnight at 20 °C. The purification procedure was as described above.

NMR spectroscopy

Two-dimensional ^{15}N-^{1}H TROSY[54] spectra were recorded at 298 K on a Bruker Avance III HD 850 MHz spectrometer equipped with a TCI-Z-GRAD cryoprobe on a sample of 150-200 µM [^{15}N]-Leu EGCII in McIlvaine's buffer [110 mM Na_2HPO_4 and 40 mM citric acid (pH 5.5)] and 6% D_2O. Data were processed with Topspin (Bruker Biospin) and analyzed using the Sparky software package[55].

EGCII activity assay and cyclophellitol complex formation

The enzymatic activity of the purified enzyme was measured in the presence of the substrate 4-methylumbelliferyl-β-D-lactopyranoside (4MU-Lac) (Marker Gene Technologies, Inc.). The enzyme (153 nM) was incubated with different concentrations of 4MU-Lac for 1 h at 37 °C in McIlvaine's (citrate/phosphate) buffer and 0.1% BSA. The reaction was quenched by adding 2.5 mL of a 0.3 M glycine solution (pH 10.6). The reaction rates were monitored by measuring the fluorescence of the released 4MU at its emission wavelength of 445 nm on an LS55 fluorimeter. For each enzymatic reaction, a blank was used, in the absence of EGCII, to measure the spontaneous hydrolysis of 4MU-Lac, and this rate was subtracted from the enzymatically catalyzed reaction rate. For covalent complex formation, EGCII and the irreversible inhibitors were incubated at a ratio of 1:30 in McIlvaine's buffer for 3 h at 25 °C. Thereafter, the samples were incubated for 1 h at 37 °C as a final step to promote complex formation and to discard aggregated protein. The samples were centrifuged for 30 min at 16000*g*, and the excess of inhibitor was removed by buffer exchange. The samples were kept at 4 °C for further experiments.

Circular dichroism (CD) spectroscopy

The far-UV region (200−280 nm) CD spectra were recorded in a 0.1 cm path length quartz cuvette in a Jasco 810 CD spectrometer using a 5 µM protein solution. The spectra were recorded using four scans with a bandwidth and a wavelength step of 1 nm. The obtained spectra were background corrected and smoothed using Jasco Spectra Manager. The unfolding transition point (T_m) was measured by following the dichroic signal decay at 222 nm, by applying heating rates from 1 to 5 °C/min, over a temperature gradient from 20 to 80 °C in McIlvaine's buffer. The obtained CD ellipticity at each point (θ_t) was assumed to be the linear combination of the folded (θ_F) and unfolded (θ_U) ellipticity. At each point of the melting curve, the unfolded fraction was calculated using the formula $f_U = (\theta_t-\theta_F)/(\theta_U-\theta_F)$. The unfolding transition curves were plotted and fitted using GraphPad Prism, and the T_m was extracted from the obtained fits as the temperature for which $f_U = 0.5$.

Limited proteolysis

Proteolysis of free EGCII and EGCII complexes was conducted at 25 or 37 °C using a trypsin: EGCII ratio of 1:100 (by weight) in the absence and the presence of 1% Triton X-100 and lauryl glucoside. A time course analysis of the proteolytic events was conducted using SDS-PAGE, and the peptic fragments were further analyzed by in-gel

digestion LC-MS on a Thermo LTQ-orbitrap mass spectrometer following the described protocol[56]. To analyze the mass of the produced EGCII tryptic fragments, the proteolytic reaction was quenched by adding phenylmethanesulfonyl fluoride (PMSF) after incubation for 10 min and analyzed on a SYNAPT G2-Si mass spectrometer (Waters).

EGCII solvent-accessible hydrophobic surface determination by 8-anilino-1-naphthalenesulfonic acid (ANSA)

Protein surface hydrophobicity was determined using ANSA according to the method described by Kato and Nakai[57]. A stock solution of 10 mM ANSA was prepared in McIlvaine's buffer. A variable amount of EGCII or EGCII-inactivator complex was mixed with a 2 mM ANSA solution. The mixture was incubated for 30 min in the dark at room temperature. The fluorescence was measured using an LS55 fluorimeter. The excitation and emission slits were both 5 nm, and the excitation and emission wavelengths were set at and 366 and 490 nm, respectively. The fluorescence of a blank solution was subtracted from each protein sample. The slope of the net fluorescence intensity (percent) plotted versus the protein concentration was calculated by linear regression analysis with GraphPad Prism and used as an index of the protein surface hydrophobicity.

Size exclusion chromatography and multiangle laser light scattering

Size exclusion chromatography in con- junction with multiangle laser light scattering (SEC-MALLS) was used to determine the absolute molecular mass of EGCII samples. EGCII (1 mg/mL) in 20 mM Tris-HCl (pH 7.6) or McIlvaine's buffer was injected into the column. The refractive index and multiangle light scattering were measured simultaneously as the solute eluted from the size exclusion column. The concentration of the solute was determined from the refractive index, the excess Rayleigh scattering from the light scattering. These two parameters were entered into the Rayleigh-Gans- Debye approximation to determine the molar mass of the solute using SEC−MALLS Astra 473 software manager[58].

References

1. Ito, M., and Yamagata, T. (1986) A novel glycosphingolipid-degrading enzyme cleaves of the linkage between the oligosaccharide and ceramide of neutral and acidic glycospingolipids. J. Biol. Chem. 261, 14278−14282.
2. Li, S.-C., Degasperi, R., Muldrey, J. E., and Li, Y.-T. (1986) A unique glycosphingolipid-splitting enzyme (ceramide-glycanase from leech) cleaves the linkage between the oligosaccharide and the ceramide. Biochem. Biophys. Res. Commun. 141, 346−352.
3. Li, Y.-T., Ishikawa, Y., and Li, S.-C. (1987) Occurrence of ceramide- glycanase in the earthworm, Lumbricusterrestris. Biochem. Biophys. Res. Commun. 149, 167−172.
4. Basu, M., Dastgheib, S., Girzadas, M. A., O'Donnell, P. H., Westervelt, C. W., Li, Z. X., Inokuchi, J., and Basu, S. (1998) Hydrophobic nature of mammalian ceramide glycanases: Purified from rabbit and rat mammary tissues. Acta Biochim. Polym. 45, 327−342.
5. Basu, M., Kelly, P., Odonell, P., Miguel, M., and Basu, S. (1998) Ceramide glycanase activities in human cancer cells. Glycobiology 8, 1129−1129.
6. Lieberman, R. L., Wustman, B. A., Huertas, P., Powe, A. C., Pine, C. W., Khanna, R., Schlossmacher, M. G., Ringe, D., and Petsko, G. A. (2007) Structure of acid [beta]-glucosidase with pharmacological chaperone provides insight into Gaucher disease. Nat. Chem. Biol. 3, 101−107.
7. Khanna, R., Benjamin, E. R., Pellegrino, L., Schilling, A., Rigat, B. A., Soska, R., Nafar, H., Ranes, B. E., Feng, J., Lun, Y., Powe, A. C., Palling, D. J., Wustman, B. A., Schiffmann, R., Mahuran, D. J., Lockhart, D. J., and Valenzano, K. J. (2010) The pharmacological chaperone isofagomine increases the activity of the Gaucher disease L444P mutant form of β-glucosidase. FEBS J. 277, 1618−1638.
8. Koshland, D. E. (1953) Stereochemistry and the mechanism of enzymatic reactions. Biol. Rev. Camb. Philos. Soc. 28, 416−436.
9. Davies, G. J., Planas, A., and Rovira, C. (2012) Conformational Analyses of the Reaction Coordinate of Glycosidases. Acc. Chem. Res. 45, 308−316.
10. Atsumi, S., Umezawa, K., Iinuma, H., Naganawa, H., Nakamura, H., Iitaka, Y., and Takeuchi, T. (1990) Production, isolation and structure determination of a novel beta-glucosidase inhibitor, cyclo- phellitol, from phellinus sp. J. Antibiot. 43, 49−53.
11. Witte, M. D., Kallemeijn, W. W., Aten, J., Li, K.-Y., Strijland, A., Donker-Koopman, W. E., van den Nieuwendijk, A. M. C. H., Bleijlevens, B., Kramer, G., Florea, B. I., Hooibrink, B., Hollak, C. E. M., Ottenhoff, R., Boot, R. G., van der Marel, G. A., Overkleeft, H. S., and Aerts, J. M. F.G. (2010) Ultrasensitive in situ visualization of active glucocerebrosidase molecules. Nat. Chem. Biol. 6, 907−913.
12. Li, K.-Y., Jiang, J., Witte, M. D., Kallemeijn, W. W., Donker- Koopman, W. E., Boot, R. G., Aerts, J. M. F. G., Codee, J. D. C., van der Marel, G. A., and Overkleeft, H. S. (2014) Exploring functional cyclophellitol analogues as human retaining β-glucosidase inhibitors. Org. Biomol. Chem. 12, 7786−7791.
13. Kallemeijn, W. W., Li, K.-Y., Witte, M. D., Marques, A. R. A., Aten, J., Scheij, S., Jiang, J., Willems, L. I., Voorn-Brouwer, T. M., van Roomen, C. P. A. A., Ottenhoff, R., Boot, R. G., van den Elst, H., Walvoort, M. T. C., Florea, B. I., Codee, J. D. C., van der Marel, G. A., Aerts, J. M. F. G., and Overkleeft, H. S. (2012) Novel Activity-Based Probes for Broad-Spectrum Profiling of Retaining beta-Exoglucosidases In Situ and In Vivo. Angew. Chem., Int. Ed. 51, 12529−12533.
14. Grabowski, G. A., Osiecki-Newman, K., Dinur, T., Fabbro, D., Legler, G., Gatt, S., and Desnick, R. J. (1986) Human acid β-glucosidase. Use of conduritol B epoxide derivatives to investigate the catalytically active normal and Gaucher disease enzymes. J. Biol. Chem. 261, 8263−8269. Brumshtein, B., Greenblatt, H. M., Butters, T. D., Shaaltiel, Y.,
15. Aviezer, D., Silman, I., Futerman, A. H., and Sussman, J. L. (2007) Crystal Structures of Complexes of N-Butyl- and N-Nonyl-Deoxynojir- imycin Bound to Acid β-Glucosidase: Insights into the mechanism of chemical chaperone action in gaucher disease. J. Biol. Chem. 282, 29052−29058.
16. Ito, M., and Yamagata, T. (1989) Purification and characterization of glycosphingolipid-specific endoglycosidases (endoglycoceramidases) from a mutant strain of *rhodococcus* sp evidence for 3 molecular-species of endoglycoceramidase with different specificities. J. Biol. Chem. 264, 9510−9519.
17. Hubbard, S. J., Eisenmenger, F., and Thornton, J. M. (1994) Modelling studies of the change in conformation required for cleavage of limited proteolytic sites. Protein Sci. 3, 757−768.
18. Zhang, N., and Li, L. (2004) Effects of common surfactants on protein digestion and matrix-assisted laser desorption/ionization mass spectrometric analysis of the digested peptides using two-layer sample preparation. Rapid Commun. Mass Spectrom. 18, 889−896.

19. Caines, M. E. C., Vaughan, M. D., Tarling, C. A., Hancock, S. M., Warren, R. A. J., Withers, S. G., and Strynadka, N. C. J. (2007) Structural and mechanistic analyses of endo-glycoceramidase II, a membrane-associated family 5 glycosidase in the Apo and GM3 ganglioside-bound forms. J. Biol. Chem. 282, 14300−14308.
20. Corbett, R. J. T., and Roche, R. S. (1984) Use of high-speed size-exclusion chromatography for the study of protein folding and stability. Biochemistry 23, 1888−1894.
21. Uversky, V. N., and Ptitsyn, O. B. (1994) Partly folded state, a new equilibrium state of protein molecules-4-state guanidinium chloride induced unfolding of beta-lactamase at low-temperature. Biochemistry 33, 2782−2791.
22. Zavodszky, P., Kardos, J., Svingor, A., and Petsko, G. A. (1998) Adjustment of conformational flexibility is a key event in the thermal adaptation of proteins. Proc. Natl. Acad. Sci. U. S. A. 95, 7406−7411.
23. Hajdu, I., Bothe, C., Szilagyi, A., Kardos, J., Gal, P., and Zavodszky, P. (2008) Adjustment of conformational flexibility of glyceraldehyde-3-phosphate dehydrogenase as a means of thermal adaptation and allosteric regulation. Eur. Biophys. J. 37, 1139−1144.
24. Thompson, P. A., Wang, S., Howett, L. J., Wang, M.-M., Patel, R., Averill, A., Showalter, R. E., Li, B., and Appleman, J. R. (2008) Identification of Ligand Binding by Protein Stabilization: Comparison of ATLAS with Biophysical and Enzymatic Methods. Assay Drug Dev. Technol. 6, 69−81.
25. Senisterra, G., Chau, I., and Vedadi, M. (2012) Thermal Denaturation Assays in Chemical Biology. Assay Drug Dev. Technol. 10, 128−136.
26. Fedorov, O., Marsden, B., Pogacic, V., Rellos, P., Müller, S., Bullock, A. N., Schwaller, J., Sundström, M., and Knapp, S. (2007) A systematic interaction map of validated kinase inhibitors with Ser/Thr kinases. Proc. Natl. Acad. Sci. U. S. A. 104, 20523−20528.
27. Carver, T. E., Bordeau, B., Cummings, M. D., Petrella, E. C., Pucci, M. J., Zawadzke, L. E., Dougherty, B. A., Tredup, J. A., Bryson, J. W., Yanchunas, J., Doyle, M. L., Witmer, M. R., Nelen, M. I., DesJarlais, R. L., Jaeger, E. P., Devine, H., Asel, E. D., Springer, B. A., Bone, R., Salemme, F. R., and Todd, M. J. (2005) Decrypting the Biochemical Function of an Essential Gene from *Streptococcus pneumoniae* Using Thermo- Fluor® Technology. J. Biol. Chem. 280, 11704−11712.
28. Teague, S. J. (2003) Implications of protein flexibility for drug discovery. Nat. Rev. Drug Discovery 2, 527−541.
29. Gonzalez, M., Bagatolli, L. A., Echabe, I., Arrondo, J. L. R., Argarana, C. E., Cantor, C. R., and Fidelio, G. D. (1997) Interaction of biotin with streptavidin - Thermostability and conformational changes upon binding. J. Biol. Chem. 272, 11288−11294.
30. Celej, M. S., Montich, C. G., and Fidelio, G. D. (2003) Protein stability induced by ligand binding correlates with changes in protein flexibility. Protein Sci. 12, 1496−1506.
31. Vedadi, M., Niesen, F. H., Allali-Hassani, A., Fedorov, O. Y., Finerty, P. J., Wasney, G. A., Yeung, R., Arrowsmith, C., Ball, L. J., Berglund, H., Hui, R., Marsden, B. D., Nordlund, P., Sundstrom, M., Weigelt, J., and Edwards, A. M. (2006) Chemical screening methods to identify ligands that promote protein stability, protein crystallization, and structure determination. Proc. Natl. Acad. Sci. U. S. A. 103, 15835−15840.
32. Andreotti, G., Monticelli, M., and Cubellis, M. V. (2015) Looking for protein stabilizing drugs with thermal shift assay. Drug Test. Anal. 7, 831−834.
33. Chaudhuri, T. K., and Paul, S. (2006) Protein-misfolding diseases and chaperone-based therapeutic approaches. FEBS J. 273, 1331−1349.
34. Andreotti, G., Citro, V., Correra, A., and Cubellis, M. V. (2014) A thermodynamic assay to test pharmacological chaperones for Fabry disease. Biochim. Biophys. Acta, Gen. Subj. 1840, 1214−1224.
35. Parenti, G., Fecarotta, S., Marca, G. l., Rossi, B., Ascione, S., Donati, M. A., Morandi, L. O., Ravaglia, S., Pichiecchio, A., Ombrone, D., Sacchini, M., Pasanisi, M. B., Filippi, P. D., Danesino, C., Della Casa, R., Romano, A., Mollica, C., Rosa, M., Agovino, T., Nusco, E., Porto, C., and Andria, G. (2014) A Chaperone Enhances Blood Alph-Glucosidase Activity in Pompe Disease Patients Treated with Enzyme Replacement Therapy. Mol. Ther., DOI: 10.1038/mt.2014.138.
36. Andreotti, G., Cabeza de Vaca, I., Poziello, A., Monti, M. C., Guallar, V., and Cubellis, M. V. (2014) Conformational Response to Ligand Binding in Phosphomannomutase2: Insights into inborn glycosylation disorder. J. Biol. Chem. 289, 34900−34910.
37. Jmoudiak, M., and Futerman, A. H. (2005) Gaucher disease: pathological mechanisms and modern management. Br. J. Haematol. 129, 178−188.
38. Lieberman, R. L., Wustman, B. A., Huertas, P., Powe, A. C., Pine, C. W., Khanna, R., Schlossmacher, M. G., Ringe, D., and Petsko, G. A. (2007) Structure of acid β-glucosidase with pharmacological chaperone provides insight into Gaucher disease. Nat. Chem. Biol. 3, 101−107.

39. Sawkar, A. R., Cheng, W. C., Beutler, E., Wong, C. H., Balch, W. E., and Kelly, J. W. (2002) Chemical chaperones increase the cellular activity of N370S β-glucosidase: A therapeutic strategy for Gaucher disease. Proc. Natl. Acad. Sci. U. S. A. 99, 15428−15433.
40. Abian, O., Alfonso, P., Velazquez-Campoy, A., Giraldo, P., Pocovi, M., and Sancho, J. (2011) Therapeutic Strategies for Gaucher Disease: Miglustat (NB-DNJ) as a Pharmacological Chaperone for Glucocerebrosidase and the Different Thermostability of Velaglucerase Alfa and Imiglucerase. Mol. Pharmaceutics 8, 2390−2397.
41. Sawkar, A. R., Adamski-Werner, S. L., Cheng, W. C., Wong, C. H., Beutler, E., Zimmer, K. P., and Kelly, J. W. (2005) Gaucher disease- associated glucocerebrosidases show mutation-dependent chemical chaperoning profiles. Chem. Biol. 12, 1235−1244.
42. Tong, M. K., and Ganem, B. (1988) A potent new class of active- site-directed glycosidase inactivators. J. Am. Chem. Soc. 110, 312−313.
43. Caron, G., and Withers, S. G. (1989) Conduritol aziridine: A new mechanism-based glucosidase inactivator. Biochem. Biophys. Res. Commun. 163, 495−499.
44. Nakata, M., Chong, C., Niwata, Y., Toshima, K., and Tatsuta, K. (1993) A family of cyclophellitol analogs: Synthesis and evaluation. J. Antibiot. 46, 1919−1922.
45. Gloster, T. M., Madsen, R., and Davies, G. J. (2007) Structural basis for cyclophellitol inhibition of a β-glucosidase. Org. Biomol. Chem. 5, 444−446.
46. Kokkinidis, M., Glykos, N. M., and Fadouloglou, V. E. (2012) Protein flexibility and enzymatic catalysis. In Advances in Protein Chemistry and Structural Biology (Christov, C., and Karabencheva Christova, T., Eds.) Vol. 87, pp 181−218, Elsevier, Amsterdam.10.1016/ B978-0-12-398312-1.00007-X.
47. Fontana, A., Polverino de Laureto, P., DeFilippis, V., Scaramella, E., and Zambonin, M. (1997) Probing the partly folded states of proteins by limited proteolysis. Folding Des. 2, R17−R26.
48. Ito, M., Ikegami, Y., and Yamagata, T. (1991) Activator proteins for glycosphingolipid hydrolysis by endoglycoceramidase: Elucidation of biological functions of cell-surface glycosphingolipids insitu by endoglycoceramidases made possible using these activator proteins. J. Biol. Chem. 266, 7919−7926.
49. Oefner, C., Binggeli, A., Breu, V., Bur, D., Clozel, J. P., D'Arcy, A., Dorn, A., Fischli, W., Gruninger, F., Guller, R., Hirth, G., Marki, H. P., Mathews, S., Muller, M., Ridley, R. G., Stadier, H., Vieira, E., Wilhelm, M., Winkler, F. K., and Wostl, W. (1999) Renin inhibition by substituted piperidines: a novel paradigm for the inhibition of monomeric aspartic proteinases? Chem. Biol. 6, 127−131.
50. Poon, D. K. Y., Ludwiczek, M. L., Schubert, M., Kwan, E. M., Withers, S. G., and McIntosh, L. P. (2007) NMR spectroscopic characterization of a β-(1,4)-glycosidase along its reaction pathway: Stabilization upon formation of the glycosyl-enzyme intermediate. Biochemistry 46, 1759−1770.
51. Jiang, J., Beenakker, T. J. M., Kallemeijn, W. W., van der Marel, G. A., van den Elst, H., Codeé, J. D. C., Aerts, J. M. F. G., and Overkleeft, H.S. (2015) Comparing Cyclophellitol N-Alkyl and N-Acyl Cyclophellitol Aziridines as Activity-Based Glycosidase Probes. Chem. Eur. J. 21, 10861−10869.
52. Li, K. Y., Jiang, J. B., Witte, M. D., Kallemeijn, W. W., van den Elst, H., Wong, C. S., Chander, S. D., Hoogendoorn, S., Beenakker, T. J. M., Codee, J. D. C., Aerts, J., van der Marel, G. A., and Overkleeft, H. S. (2014) Synthesis of Cyclophellitol, Cyclophellitol Aziridine, and Their Tagged Derivatives. Eur. J. Org. Chem. 2014, 6030−6043.
53. Senn, H., Eugster, A., Otting, G., Suter, F., and Wüthrich, K. (1987) 15N-labeled P22 c2 repressor for nuclear magnetic resonance studies of protein-DNA interactions. Eur. Biophys. J. 14, 301−306.
54. Pervushin, K., Riek, R., Wider, G., and Wüthrich, K. (1997) Attenuated T2 relaxation by mutual cancellation of dipole-dipole coupling and chemical shift anisotropy indicates an avenue to NMR structures of very large biological macromolecules in solution. Proc. Natl. Acad. Sci. U. S. A. 94, 12366−12371.
55. Goddard, T. D., and Kneller, D. G. (2007) SPARKY 3, University of California, San Francisco.
56. Shevchenko, A., Tomas, H., Havlis, J., Olsen, J. V., and Mann, M. (2007) In-gel digestion for mass spectrometric characterization of proteins and proteomes. Nat. Protoc. 1, 2856−2860.
57. Kato, A., and Nakai, S. (1980) Hydrophobicity determined by a fluorescence probe method and its correlation with surface-properties of proteins. Biochim. Biophys. Acta, Protein Struct. 624, 13−20.
58. Knobloch, J. E., and Shaklee, P. N. (1997) Absolute molecular weight distribution of low-molecular-weight heparins by size-exclusion chromatography with multiangle laser light scattering detection. Anal. Biochem. 245, 231−241.
59. Ye, Y., and Godzik, A. (2003) Flexible structure alignment by chaining aligned fragment pairs allowing twists. Bioinformatics 19, ii246− ii255.

60. Oberhauser, N., Nurisso, A., and Carrupt, P.-A. (2014) MLP Tools: a PyMOL plugin for using the molecular lipophilicity potential in computer-aided drug design. J. Comput.-Aided Mol. Des. 28, 587−596.